Journal of Power Sources 270 (2014) 359–366

Contents lists available at ScienceDirect

Journal of Power Sources

journal homepage: www.elsevier.com/locate/jpowsour

A novel method for state of charge estimation of lithium-ion batteries using a nonlinear observer

Bizhong Xia [a], Chaoren Chen [a], Yong Tian [a, *], Wei Sun [b], Zhihui Xu [b], Weiwei Zheng [b]

[a] Graduate School at Shenzhen, Tsinghua University, Shenzhen, Guangdong 518055, China
[b] Sunwoda Electronic Co. Ltd., Shenzhen, Guangdong 518108, China

HIGHLIGHTS

- A novel method for SOC estimation using a nonlinear observer is presented.
- State equations are derived from the first-order RC equivalent circuit model.
- The observer for SOC estimation is designed and its convergence is proved.
- The new method has merits in computation cost, accuracy and convergence rate.

ARTICLE INFO

Article history:
Received 17 May 2014
Received in revised form
15 July 2014
Accepted 16 July 2014
Available online 24 July 2014

Keywords:
State of charge
Nonlinear observer
Lithium-ion battery
Electric vehicles

ABSTRACT

The state of charge (SOC) is important for the safety and reliability of battery operation since it indicates the remaining capacity of a battery. However, as the internal state of each cell cannot be directly measured, the value of the SOC has to be estimated. In this paper, a novel method for SOC estimation in electric vehicles (EVs) using a nonlinear observer (NLO) is presented. One advantage of this method is that it does not need complicated matrix operations, so the computation cost can be reduced. As a key step in design of the nonlinear observer, the state–space equations based on the equivalent circuit model are derived. The Lyapunov stability theory is employed to prove the convergence of the nonlinear observer. Four experiments are carried out to evaluate the performance of the presented method. The results show that the SOC estimation error converges to 3% within 130 s while the initial SOC error reaches 20%, and does not exceed 4.5% while the measurement suffers both 2.5% voltage noise and 5% current noise. Besides, the presented method has advantages over the extended Kalman filter (EKF) and sliding mode observer (SMO) algorithms in terms of computation cost, estimation accuracy and convergence rate.

© 2014 Elsevier B.V. All rights reserved.

1. Introduction

Electric vehicles (EVs), including pure electric vehicle (PEV), hybrid electric vehicle (HEV) and fuel cell electric vehicle (FCEV) are considered to be an effective way to ease energy crisis and environmental pollution. Comparing with other batteries, such as lead-acid battery and nickel–cadmium battery, lithium-ion battery (LIB) has been widely used in EVs due to its higher energy and power density, lower self-discharging rate and longer cycle life. However, LIB has higher requirements for the battery management system (BMS). For example, it has greater risk of burning or exploding than other batteries if it is over-charged or over-discharged. Estimating the SOC is one of the most key techniques in the design of BMS, especially for those used in EVs. An accurate SOC estimation approach will improve the efficiency of power distribution, extend the battery cycle life and prevent the battery from over-charging or over-discharging. Nevertheless, it is difficult to get an accurate value of SOC, because the SOC cannot be measured directly and its value is affected by various factors, such as the current, temperature and cycles (aging).

A number of methods have been proposed to estimate the SOC, such as the ampere-hour (Ah) counting, Kalman filter (KF), sliding mode observer (SMO), particle filter (PF), artificial neural network (ANN) and fuzzy logic (FL) methods. The Ah counting method [1] is the most common one and usually used as the basis of other methods. The merit of Ah method is that it is simple and easy to implement. However, it suffers accumulated errors from the integration process due to inaccurate measurement current.

* Corresponding author. Tel.: +86 755 26036757.
E-mail address: tian.yong@sz.tsinghua.edu.cn (Y. Tian).

http://dx.doi.org/10.1016/j.jpowsour.2014.07.103
0378-7753/© 2014 Elsevier B.V. All rights reserved.

Furthermore, as an open-loop estimation method, it cannot deal with the initial SOC error problem. The original KF is a linear estimation method. To expand its application in the nonlinear battery systems, the extended Kaman filter (EKF) [2–7] and unscented Kalman filter (UKF) [8,9] have been developed. Both the EKF and UKF methods can estimate the SOC accurately if the battery model is accurate enough and the system is not highly nonlinear. However, they have poor applicability for highly nonlinear systems and have high requirements for hardware due to a large number of matrix operations. Furthermore, the KF method is based on an assumption that the noise is Gaussian white noise and the statistical property of the noise should be known before the SOC is estimated. However, this usually cannot be met in practice. The SMO [10,11] is a reliable and robust method for SOC estimation in terms of model error and external disturbance. However, it is difficult to design the SMO for SOC estimation because the optimal parameters are hard to obtain. The PF [12] method also needs numerous matrix operations and has high requirements for hardware. The ANN method [13–15] requires a large number of sample data and a reliable learning algorithm. The FL method [16] is difficult to design and its performance depends on the designer's experience.

In this paper, a novel method for SOC estimation using a nonlinear observer is presented. This method does not need complicated matrix operations and is robust against the measurement errors and parameter uncertainties. Comparing with EKF method, the presented method can reduce the computation cost with the similar SOC estimation accuracy and convergence performance. Comparing with SMO method, it can improve the SOC estimation accuracy and accelerate convergence simultaneously. Therefore, the proposed method has good performance and can be easily implemented in an online estimation system.

The remains of this paper are organized as follows. Section 2 introduces the first-order resistor–capacitor battery equivalent circuit model, based on which the state-space equations are derived. Section 3 illustrates the design of the nonlinear observer for the SOC estimation and proves the convergence of the observer. Section 4 shows the experimental configurations. Experimental results and discussion are presented in Section 5. Finally, Section 6 concludes the paper.

2. Battery modeling

2.1. Equivalent circuit model of a battery

A common definition of SOC is formulated as.

$$\mathrm{SOC}(t) = \mathrm{SOC}(t_0) - \frac{\int_{t_0}^{t} i\mathrm{d}t}{C_n} \tag{1}$$

Based on Eq. (1), the derivative of SOC can be obtained as.

$$\dot{\mathrm{SOC}}(t) = -\frac{i(t)}{C_n} \tag{2}$$

where i represents the battery current, whose value is positive while discharging and negative while charging; and C_n is the battery nominal capacity.

An accurate battery model that can simulate the dynamic characteristic of a LIB is essential to the SOC estimation. Therefore, many battery models have been proposed, among which the most common are the equivalent circuit models, including the resistor model [9], first-order resistor–capacitor (RC) model [17–19], second-order RC model [3,11] and complicated RC models [20–22]. The resistor model is the simplest model and has the lowest computation cost. However it cannot accurately reflect the dynamic voltage characteristic of a battery. The complicated electrical models can reduce model errors, but increase system complexity and computation cost. In Refs. [19], a comparative study of twelve equivalent circuit models for LIB was presented. The results indicate that the first-order RC model is a good choice to balance between model robustness and complexity since it is almost as good as more complex models. Therefore, in this paper, the first-order RC model is utilized to make a trade-off between the model error and computation cost. As shown Fig. 1, the first-order RC model consists of an open-circuit voltage $U_{\mathrm{oc}}(\mathrm{SOC})$, a resistor R_o, and an RC network R_1 and C_1. The resistor R_o is used to represent the electrical resistance of battery components with the accumulation and dissipation of charge in the electrical double-layer, and it is called as ohmic resistance. While the RC network is employed to describe the mass transport effects and dynamic voltage performance, the elements of R_1 and C_1 are accordingly called as the diffusion resistance and diffusion capacitance, respectively [5].

The electrical behavior of the first-order RC model can be expressed as.

$$\dot{U}_1 = -\frac{U_1}{R_1 C_1} + \frac{I_L}{C_1} \tag{3}$$

$$U_L = U_{\mathrm{oc}}(\mathrm{SOC}) - U_1 - I_L R_o \tag{4}$$

where U_1 is the terminal voltage of capacitor C_1, U_L is the load voltage, and I_L is the load current.

2.2. Model parameters identification

For the first-order RC equivalent circuit model shown in Fig. 1, the values of parameters R_o, R_1 and C_1, as well as the relationship expression between the open circuit voltage (OCV) and the SOC have to be identified. To do so, pulse discharge experiment has been carried out based on the ICR18650–22F typed lithium-ion batteries. More details about the battery parameters and the test bench configurations will be illustrated in Section 4. With the exponential-function fitting method, the values of parameters R_o, R_1 and C_1 are obtained, as shown in Table 1.

An accurate relationship expression between the OCV and the SOC is crucial to improve the SOC estimation accuracy. Various approaches have been developed to describe the relationship between the OCV and the SOC. For instance, a straight–line fitting method was used in Ref. [10], while a broken–line fitting method was utilized in Ref. [11]. Both of the two methods are simple, but not accurate enough to capture the dynamic voltage behavior of a battery. In this paper, a ninth–order polynomial fitting method is employed to improve the model accuracy. The profile of COV versus

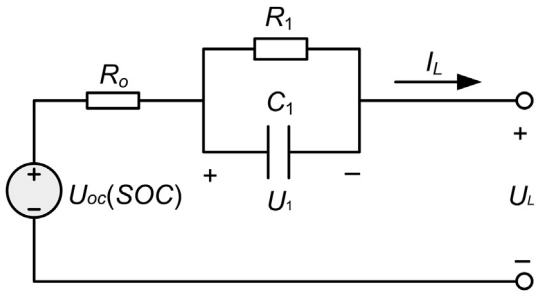

Fig. 1. Schematic diagram of the first-order RC equivalent circuit model.

Table 1
Parameters of the first-order RC equivalent circuit model.

R_o	R_1	C_1
0.0377 Ω	0.0241 Ω	2000 F

SOC is shown in Fig. 2, where marks "o" represent the experimental data, while the solid–line stands for the fitted curve. It can be seen that the ninth–order polynomial can well capture the OCV variation with SOC.

3. Design of nonlinear observer for SOC estimation

The SOC estimation for lithium-ion batteries is a nonlinear problem that can be seen from the highly nonlinear relationship between the OCV and the SOC as shown in Fig. 2. One simple method to solve the nonlinear problem is to simplify the problem by linearization. For example, a straight–line fitting method and broken–line fitting method were respectively used in Ref. [10] and in Ref. [11] to approximately describe the battery OCV–SOC relationship. With the linearization method, the computation cost is low, but it is easy to encounter large estimation error. For EKF and UKF methods, the first order or the second terms of the Taylor series expansion are utilized to approximate the nonlinear function and the high order terms are ignored, which may result in the instability of the filter and inaccurate estimation for a highly nonlinear battery system in EVs.

Observers are widely used to solve estimation problems. The essential idea of the observer–based methods is utilizing the deviation to weaken the deviation. The most key and difficult aspect to design an observer is to find the proper gain to reduce the deviation. Many observers have been proposed to solve estimation problems. The linear observers [10,11,23] are commonly used and easy to design. Several nonlinear observers [24,25] are utilized to solve conventional nonlinear problems, but they are only suitable for the nonlinear systems with a nonlinear system equation and a linear observation equation. For a battery system, a linear observation equation will lead to the increase of the SOC estimation error because the model error is enlarged. To accurately represent the model information, the observation equation should be nonlinear and the system equation should be linear. To resolve such kind of nonlinear problem, a nonlinear observer introduced in Ref. [26] is used in this paper. An important characteristic of this nonlinear observer is that the gain matrix is updated with the SOC, so it has good robustness against the external disturbance and parameter uncertainties.

Based on Eqs. (2) and (3), the system equation of a battery can be derived as.

$$\dot{x} = Ax + BI_L \tag{5}$$

where $A = \begin{bmatrix} -\tau & 0 \\ 0 & 0 \end{bmatrix}$, $\tau = 1/R_1C_1$, $B = \begin{bmatrix} 1/C_1 \\ -1/C_n \end{bmatrix}$, $x = \begin{bmatrix} U_1 \\ \mathrm{SOC} \end{bmatrix}$, and $\dot{x}$ represents the derivative of x.

Based on Eq. (4), the observation equation can be derived as.

$$U_L = h(x) - I_L R_o \tag{6}$$

$$h(x) = -U_1 + U_{oc}(\mathrm{SOC}) \tag{7}$$

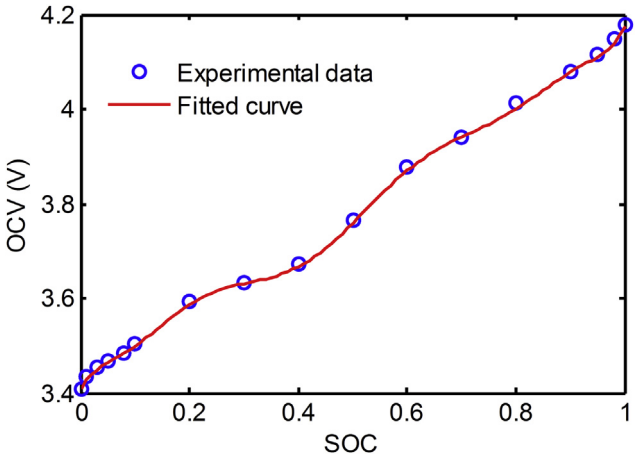

Fig. 2. Measured and fitted OCV vs. SOC.

$$\dot{h}(x) = \begin{bmatrix} \dfrac{\partial h(x)}{\partial U_1} & \dfrac{\partial h(x)}{\partial \mathrm{SOC}} \end{bmatrix} = \begin{bmatrix} -1 & \dot{U}_{oc}(\mathrm{SOC}) \end{bmatrix} \tag{8}$$

As shown above, the observation equation is nonlinear. The nonlinear observer can be designed as Eqs. (9)–(13).

$$\dot{\hat{x}} = A\hat{x} + BI_L + K\dot{h}^T(\hat{x})\left(U_L - \hat{U}_L\right) \tag{9}$$

$$\hat{U}_L = h(\hat{x}) - I_L R_0 \tag{10}$$

$$U_L - \hat{U}_L = h(x) - h(\hat{x}) = \dot{h}(\xi)(x - \hat{x}) \approx \dot{h}(\hat{x})e_x \tag{11}$$

$$e_x = x - \hat{x} \tag{12}$$

$$\dot{e}_x = Ae_x - K\dot{h}^T\dot{h}e_x = \left(A - K\dot{h}^T\dot{h}\right)e_x \tag{13}$$

where $\hat{x}$ is the observation value of x, $\hat{U}_L$ is the observation value of U_L, e_x is the observation error of x, and K is the gain matrix that can be obtained from the Lyapunov equation shown in Eq. (14).

$$A^T K^{-1} + K^{-1}A = -Q \tag{14}$$

where the rank of matrix Q is equal to that of A and the Eigenvalues of Q are always larger than zero, so both K^{-1} and K are positive definite matrixes.

By assuming $Q = \begin{bmatrix} 2b_1 & 0 \\ 0 & 0 \end{bmatrix}$, it can be deduced that $K = \begin{bmatrix} k_1\tau & 0 \\ 0 & k_2\tau \end{bmatrix}$ and $K^T = K$, where k_1 (=$1/b_1$) and k_2 are undetermined positive constants. The Lyapunov stability theory is introduced to prove the convergence of the nonlinear observer and the corresponding function is selected as,

$$V(e_x) = e_x^T K^{-1} e_x \tag{15}$$

then

$$\begin{aligned} V(e_x) &= \dot{e}_x^T K^{-1} e_x + e_x^T K^{-1}\dot{e}_x = \left(\left(A - K\dot{h}^T\dot{h}\right)e_x\right)^T K^{-1}e_x + e_x^T K^{-1}\left(\left(A - K\dot{h}^T\dot{h}\right)e_x\right) \\ &= e_x^T A^T K^{-1}e_x + e_x^T K^{-1}Ae_x - e_x^T\dot{h}^T\dot{h}KK^{-1}K^{-1}e_x - e_x^T\dot{h}^T\dot{h}KK^{-1}e_x = e_x^T\left(-Q\right)e_x - e_x^T\left(2\dot{h}^T\dot{h}\right)e_x = -e_x^T\left(Q + 2\dot{h}^T\dot{h}\right)e_x \end{aligned} \tag{16}$$

$$Q + 2\dot{h}^T\dot{h} = 2 \times \begin{bmatrix} b_1 + 1 & -\dot{U}_{oc} - \dot{U}_{oc}\dot{U}_{oc}^2 \end{bmatrix} \tag{17}$$

$$\left|Q + 2\dot{h}^T\dot{h}\right| = 4 \times \left| b_1 + 1 \quad -\dot{U}_{oc} - \dot{U}_{oc}\dot{U}_{oc}^2 \right| = 4b_1\dot{U}_{oc}^2 \tag{18}$$

As mentioned above, $(b1 + 1)$ is positive, hence,

$$\left|Q + 2\dot{h}^T\dot{h}\right| > 0 \tag{19}$$

That's to say, $Q + 2\dot{h}^T\dot{h}$ is positive definite, then,

$$\dot{V}(e_x) < 0 \tag{20}$$

Thus, $\dot{V}(e_x)$ is negative definite and the error system shown in Eq. (13) is asymptotically stable. The dynamical system in Eqs. (9) and (10) can be selected as an observer for the system in Eqs. (5) and (6). In this paper, regarding of the robustness and convergence rate of the nonlinear observer simultaneously, the values of k_1 and k_2 are chosen as 2 and 2.5, respectively.

4. Experimental configurations

The experiment setup is shown in Fig. 3. It consists of (1) lithium-ion batteries; (2) a control board for battery charge/discharge controlling, as well as battery voltage and current sampling with a period of 1 s; (3) a personal computer with monitoring software for data sampling and MATLAB R2010a for data analysis; (4) a DC contactor for charge/discharge switching; (5) a power supply and (6) a programmable electric load. The batteries used in this test are Samsung ICR18650–22F–typed lithium-ion battery, whose nominal voltage and nominal capacity are 3.62 V and 2.2 Ah, respectively. Four experiments, including (1) constant current discharge test, (2) variable current discharge test with accurate initial SOC and measurement, (3) variable current discharge test with initial SOC error and measurement noise, (4) comparison with two of the well–established algorithms are implemented on the test bench to evaluate the performance of the proposed method. The constant current discharge experiment is used to simulate the loading condition when the EV runs in a constant speed, while the variable current discharge experiment is used to simulate the condition when the EV runs in a variable speed.

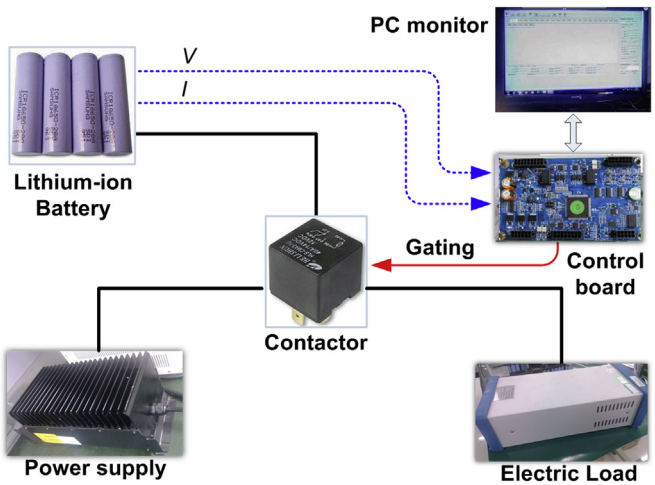

Fig. 3. Schematic diagram of the test bench.

It is noted that, in all cases, the reference SOC values are calculated by the current integral method according to measured data. To obtain an accurate reference SOC, the batteries are firstly fully charged before driving cycle test and finally fully discharged after driving cycle with a nominal current. In this way, an accurate initial SOC and a terminal SOC can be obtained.

5. Results and discussion

5.1. Experiment A: constant current discharge test

In experiment A, the battery was discharged with a constant current of 1.075 A (about 0.5 C) from the fully charged state (SOC = 1) to the state of SOC = 0.1 and the corresponding terminal voltage decreases from 4.148 V to 3.400 V, as shown in Fig. 4(a), where the blue dotted-line is the terminal voltage measured with a high precision voltage sensor and the red solid-line (in the web version) is that estimated by the nonlinear observer. This experiment aims to simulate the condition when an electric vehicle runs in a constant speed. From Fig. 4(a) it can be seen that the measured terminal voltage is smooth and without any obvious fluctuation as the current is constant. Furthermore, the estimated terminal voltage is nearly overlapped with the reference one, suggesting the maximum estimation error is less than 0.02 V, as shown in Fig. 4(b). The SOC estimation results are shown in Fig. 5(a), where the blue dotted-line (in the web version) is the reference value calculated by current integral method with an accurate initial SOC value and the red solid-line is the estimated one. The SOC estimation error is shown in Fig. 5(b), from where it can be seen that the maximum error is less than 3%.

5.2. Experiment B: AUDC test

Experiment B is used to simulate a typical loading condition when the EVs are on urban roads. The battery current profile

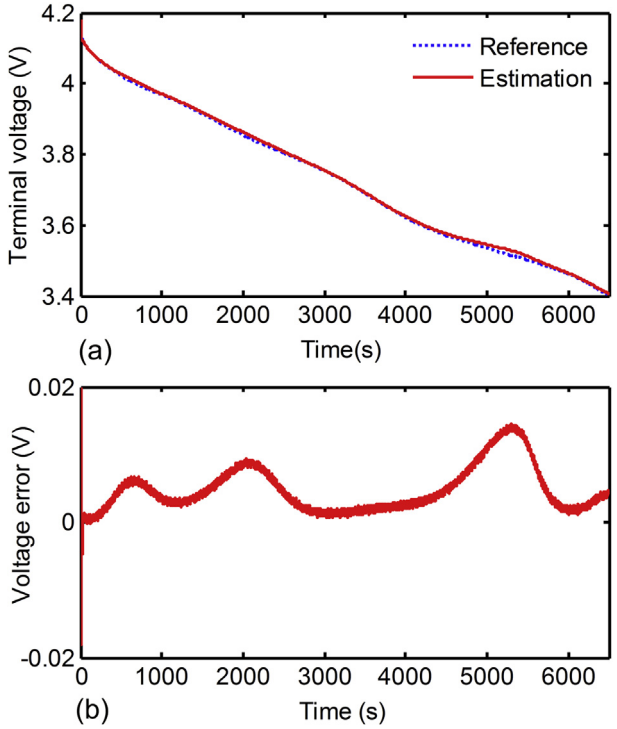

Fig. 4. Voltage estimation under constant-current test. (a) Voltage; (b) voltage error.

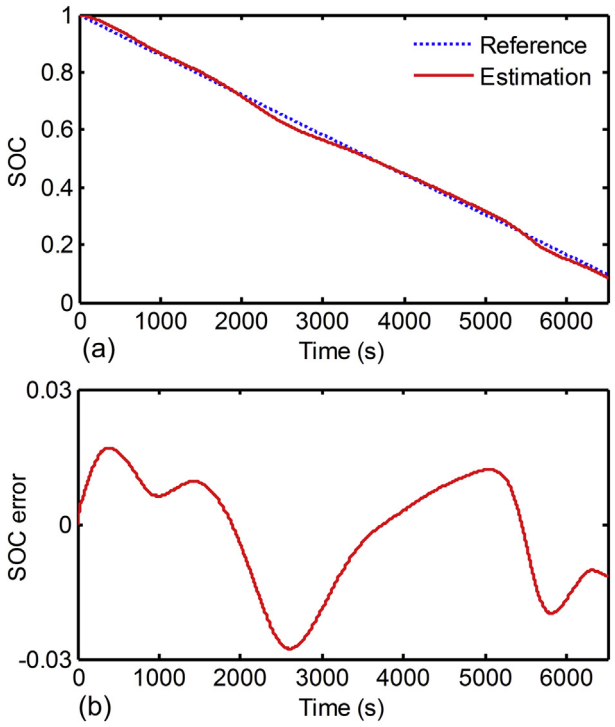

Fig. 5. SOC estimation under constant-current test. (a) SOC; (b) SOC error.

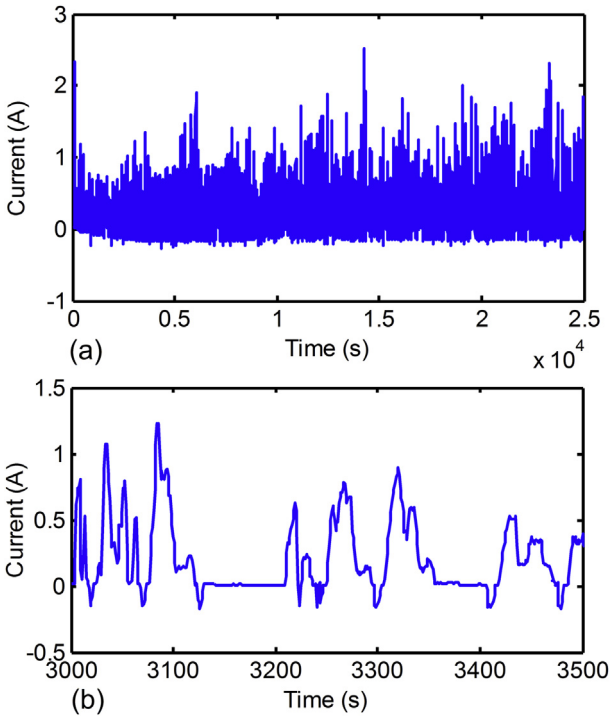

Fig. 6. Current profile under AUDC test. (a) Current vs. time profile; (b) zoom figure for (a).

collected from actual urban driving cycles (AUDC) test is shown in Fig. 6, in which the positive current represents battery discharge while the negative current stands for battery charge. The variation of the battery terminal voltage vs. time is shown in Fig. 7(a), where the blue dotted-line (in the web version) is the measured terminal voltage with a high precision voltage sensor and the red solid-line is that estimated by the nonlinear observer. It can be seen that the terminal voltage shows serious fluctuations due to the sharply variable current. Furthermore, the observation voltage fluctuates to the same degree as the measured one, and the maximum estimation error is about 0.1 V, as shown in Fig. 7(b). The SOC estimation results are shown in Fig. 8(a), where the blue dotted-line (in the web version) is the reference SOC values calculated by the current integral method with an accurate initial SOC value, while the red solid-line is the estimated ones. The SOC estimation error is shown in Fig. 8(b), from where it can be seen that the maximum error is lower than 3%. These results indicate that the proposed method has good performance in terms of terminal voltage and SOC estimation accuracy even though the battery operation current fluctuates sharply.

5.3. Experiment C: robustness evaluation

In experiments A and B, the initial SOC value is assumed to be accurate. However, the initial SOC value is not fixed due to the battery self-discharge and capacity recovery effect. Besides, it is assumed that the current and voltage are measured by high precision sensors. Thus, the measurements are considered to be accurate. However, it is difficult to always get accurate values of voltage and current for an online system due to factors, such as the electromagnetic interference (EMI) generated by electronic equipment on EVs and low precision sensors. To evaluate the robustness of the nonlinear observer against the initial SOC error and the measurement noise, experiment B was conducted repeatedly with initial SOC error and stochastic normal distributed measurement noise. The results with an initial SOC error of 20% are shown in Fig. 9. It is indicated that the estimation error converges to the range of 3% within 130 s, which proves that the proposed method is good at dealing with the initial SOC error problem.

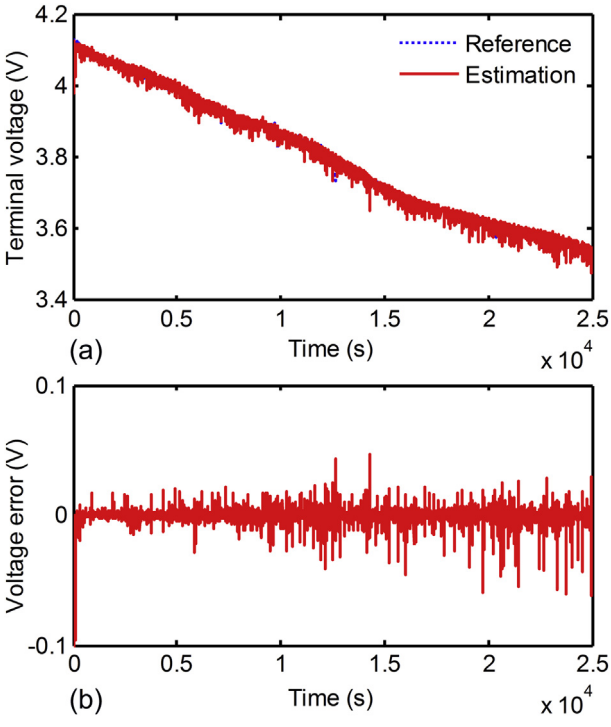

Fig. 7. Voltage estimation under AUDC test. (a) Voltage; (b) voltage error.

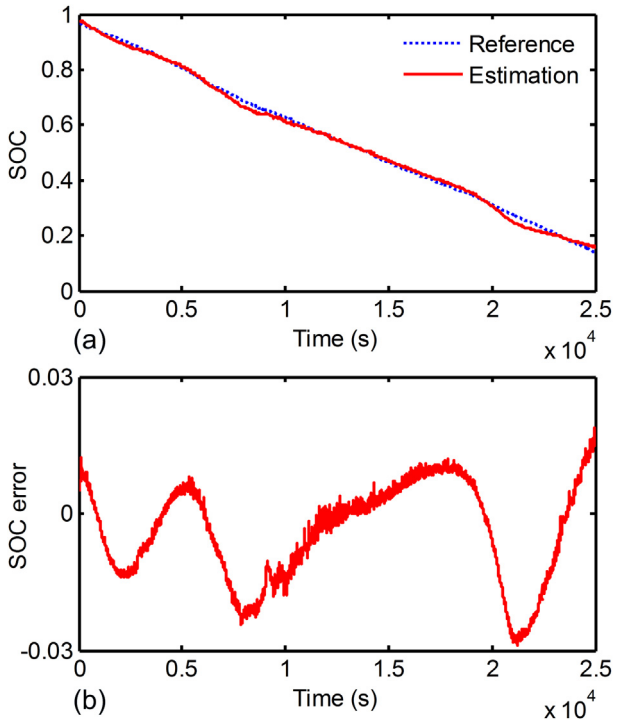

Fig. 8. SOC estimation under AUDC test. (a) SOC; (b) SOC error.

To evaluate the robustness of the proposed method against the current error, stochastic normal distributed noises were added to the measurement current shown in Fig. 6. The mean value of the noise is zero and its standard deviation can be calculated by.

$$\sigma = \frac{1}{3} p L_{\max} \tag{21}$$

where σ is the standard deviation, p is a scale factor, and $L_{\max}$ represents the maximum current or the maximum voltage. In this paper, the conditions that p = 1%, 2.5% and 5% are studied. The results of Experiment C with current noises, voltage noises, and both current and voltage noises are shown in Figs. 10–12, respectively.

In Fig. 10(a), the blue dotted-line (in the web version) is the reference SOC calculated by the current integral method with accurate initial SOC and measured current, the red solid-line shows the SOC estimated by the nonlinear observer with 5% current noise, while the blue solid-line and the black dotted-line illustrate the values with 2.5% and 1% current noises, respectively. The corresponding estimation errors are shown in Fig. 10(b), and the root mean square errors (RMSEs) and maximum errors are shown in Table 2. It can be seen that with the increase of current noise, both the RMSEs and maximum errors remain stable. Besides, the maximum errors are also within 3%, which indicates that the nonlinear observer has a good robustness against the current noise.

In Fig. 11(a), the blue dotted-line (in the web version) is the reference SOC calculated by the current integral method with an accurate initial SOC and measured voltage, the red solid-line shows the SOC estimated by the nonlinear observer with 5% voltage noise, while the blue solid-line and the black dotted-line are the SOC with 2.5% and 1% voltage noises, respectively. The corresponding estimation errors are shown in Fig. 11(b), and the corresponding RMSEs and maximum error are shown in Table 3. It can be seen that with the increase of voltage noises, the RMSEs remain stable while the maximum errors increase, which indicates that the nonlinear observer has a weaker robustness against the voltage disturbance compared with that against the current disturbance. The reason is that the highly nonlinear OCV–SOC function is the convergence basis of the nonlinear observer. Therefore, the voltage accuracy is essential to the estimation results.

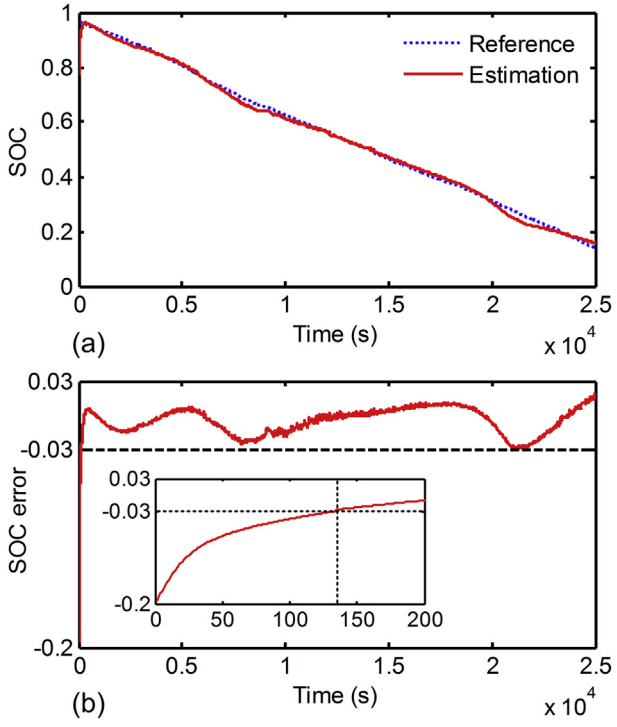

Fig. 9. SOC estimation with initial SOC error under AUDC test. (a) SOC; (b) SOC error.

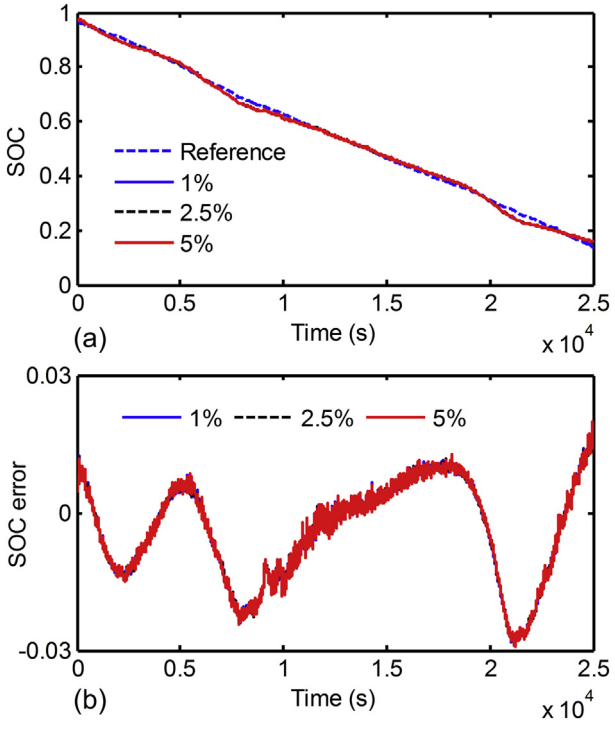

Fig. 10. SOC estimation with different current noises under AUDC test. (a) SOC; (b) SOC error.

Table 2
SOC estimation errors with different current noises under AUDC test.

Current noises factor (p)	1%	2.5%	5%
RMSEs	0.91%	0.91%	0.91%
Maximum errors	2.89%	2.90%	2.93%

Table 3
SOC estimation errors with different voltage noises under AUDC test.

Voltage noises factor (p)	1%	2.5%	5%
RMSEs	0.92%	0.95%	1.18%
Maximum errors	3.13%	3.92%	5.64%

Figs. 10 and 11 show the conditions that only current disturbance or voltage disturbance occurs. However, in online estimation, current disturbance and voltage disturbance may be generated simultaneously. Thus, the case with both current and voltage noises has also been studied in the paper. The results are shown in Fig. 12. In Fig. 12(a), the blue dotted-line is the reference SOC that is calculated by the coulomb counting method with accurate initial SOC and measured current, while the red solid-line (in the web version) is the SOC estimated by the nonlinear observer with both 2.5% voltage noise and 5% current noise. It is noted that the SOC estimation error is bounded in 4.5%, and the calculated RMSE and maximum error are 1.08% and 4.27% respectively, which meet the requirements of EVs application.

5.4. Experiment D: comparison of SOC estimation methods

To further illustrate the advantages of the proposed nonlinear observer (NLO) method, the results of experiments B and C were compared to the ones obtained by two of the well–established algorithms, namely, extended Kalman filter (EKF) and sliding mode observer (SMO). More details about EKF can be found in Refs. [2–9] and about SMO can be found in Refs. [10,11]. In this paper, three aspects, including (1) SOC estimation accuracy, (2) computation cost and (3) convergence rate are studied. The comparison results of experiment B are shown in Fig. 13 and Table 4. The comparison results of experiment C with initial SOC error are shown in Fig. 14 and Table 5. With all the comparison results, it is clear that the proposed method has similar convergence rate, but higher accuracy and less computation cost than EKF method. Besides, it has better

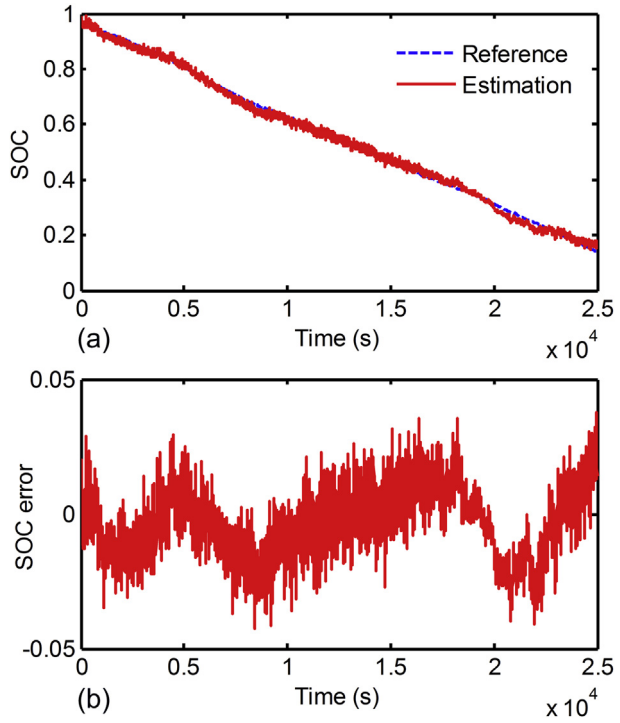

Fig. 12. SOC estimation with both current and voltage noises under AUDC test. (a) SOC; (b) SOC error.

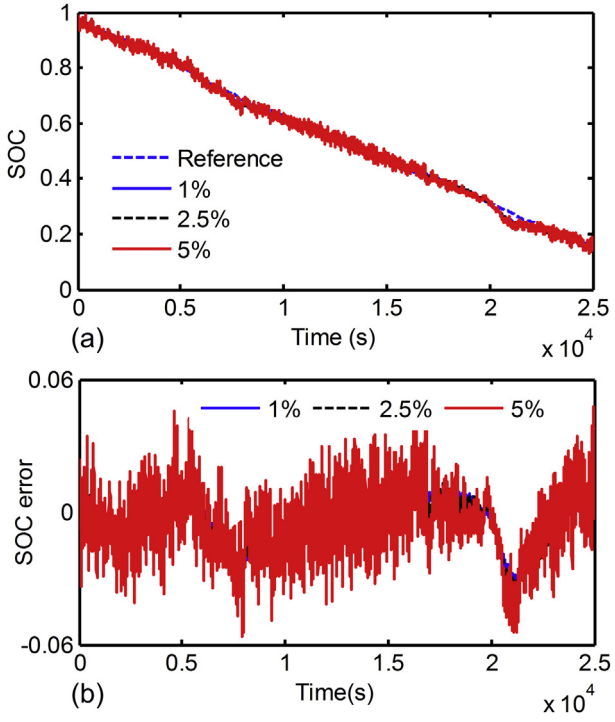

Fig. 11. SOC estimation with different voltage noises under AUDC test. (a) SOC; (b) SOC error.

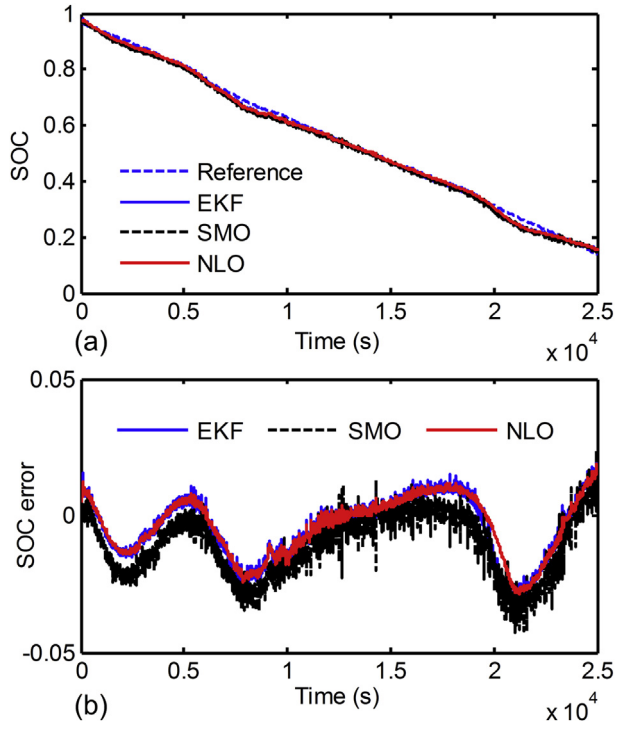

Fig. 13. Comparison of SOC estimation under AUDC test. (a) SOC; (b) SOC error.

Table 4
Comparison of computation cost and SOC estimation error under AUDC test.

Estimation methods	EKF	SMO	NLO
Computation cost	2.904 s	1.420 s	1.180 s
RMSEs	0.97%	1.17%	0.92%
Maximum errors	3.21%	4.25%	2.89%

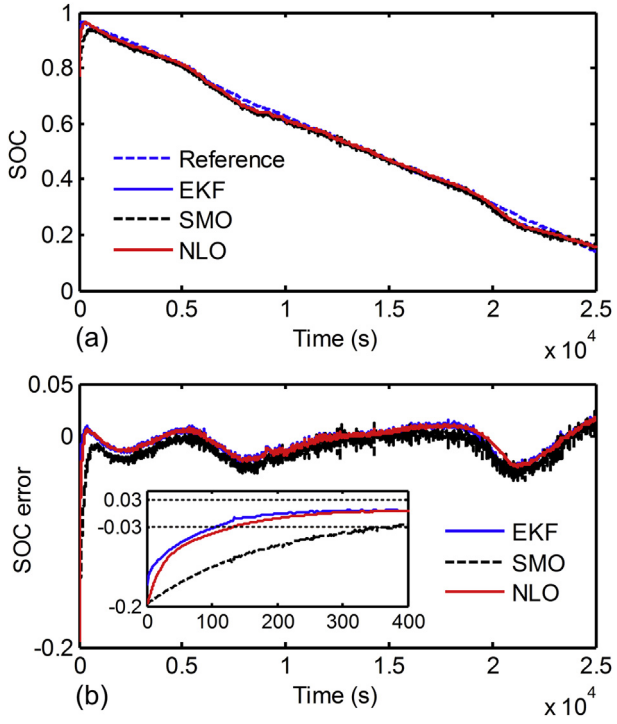

Fig. 14. Comparison of SOC estimation with initial SOC error under AUDC test. (a) SOC; (b) SOC error.

Table 5
Comparison of convergence rate and SOC estimation error with initial SOC error under AUDC test.

Estimation methods	EKF	SMO	NLO
Convergence rate	100 s	360 s	130 s
RMSEs	0.99%	1.31%	0.95%

performance at all of the three aspects compared with the SMO method.

6. Conclusions

Estimating the SOC of a lithium-ion battery is essential for the popularity of electrical vehicles. In this paper, a novel SOC estimation method using a nonlinear observer has been proposed to simultaneously reduce the computation cost and improve the SOC estimation accuracy. To make a trade-off between the model error and computation cost, the first-order RC equivalent circuit model is used to simulate the dynamic behaviors of a lithium-ion battery, based on which the state-space equations are derived. A ninth-order polynomial is utilized to describe the highly nonlinear relationship between the OCV and the SOC. To deal with the highly nonlinear problem, a nonlinear observer for SOC estimation is designed. Besides, a constant current discharge test and an actual urban driving cycles test are carried to evaluate the performance of the proposed method. The experimental results show that the SOC estimation error based on the proposed method can quickly converge to 3% within about 130 s while the initial SOC error reaches 20%. Besides, the error does not exceed 4.5% even the measurement simultaneously suffers 2.5% voltage noise and 5% current noise. Furthermore, comparison results show that the proposed method has better performance in improving accuracy, reducing computation cost and accelerating convergence than the EKF and SMO algorithms. Therefore, the proposed method is suitable for online SOC estimation.

Acknowledgments

This work is supported by the China Postdoctoral Science Foundation Funded Project (No. 2013M540941) and the Shenzhen Key Laboratory of LED Packaging Funded Project (No. NZDSY20120619141243215).

References

[1] K.S. Ng, C.S. Moo, Y.P. Chen, Y.C. Hsieh, Appl. Energy 86 (2009) 1506–1511.
[2] X. Hu, S. Li, H. Peng, F. Sun, J. Power Sources 217 (2012) 209–219.
[3] X. Long, J.P. Wang, Q.S. Chen, Energy Convers. Manage. 53 (2012) 33–39.
[4] S. Sepasi, R. Ghorbani, B.Y. Liaw, J. Power Sources 245 (2014) 337–344.
[5] R. Xiong, F.C. Sun, Z. Chen, H.W. He, Appl. Energy 113 (2014) 463–476.
[6] R. Xiong, F.C. Sun, X.Z. Gong, C.C. Gao, Appl. Energy 113 (2014) 1421–1433.
[7] C.J. Chiang, J.L. Yang, W.C. Cheng, J. Power Sources 234 (2013) 234–243.
[8] F.C. Sun, X.S. Hu, Y. Zou, S.G. Li, Energy 36 (2011) 3531–3540.
[9] W. He, N. Williard, C.C. Chen, M. Pecht, Microelectron. Reliab. 53 (2013) 840–847.
[10] I.S. Kim, J. Power Sources 163 (2006) 584–590.
[11] X.P. Chen, W.X. Shen, Z.W. Cao, A. Kapoor, J. Power Sources 246 (2014) 667–678.
[12] S. Schwunk, N. Armbruster, S. Straub, J. Kehl, M. Vetter, J. Power Sources 239 (2013) 705–710.
[13] W.X. Shen, C.C. Chan, E.W.C. Lo, K.T. Chau, Energy Convers. Manage. 43 (2002) 817–826.
[14] B. Cheng, Z. Bai, B. Cao, Energy Convers. Manage. 49 (2008) 2788–2794.
[15] I.H. Li, W.Y. Wang, S.F. Su, Y.S. Lee, IEEE Trans. Energy Convers. 22 (2007) 697–708.
[16] A.J. Salkind, C. Fennie, P. Singh, T. Atwater, D.E. Reisner, J. Power Sources 80 (1999) 293–300.
[17] V.H. Johnson, J. Power Sources 110 (2002) 321–329.
[18] S. Lee, J. Kim, J. Lee, B.H. Cho, J. Power Sources 185 (2008) 1367–1373.
[19] X. Hu, S. Li, H. Peng, J. Power Sources 198 (2012) 359–367.
[20] G.L. Plett, J. Power Sources 134 (2004) 262–276.
[21] J. Lee, O. Nam, B.H. Cho, J. Power Sources 174 (2007) 9–15.
[22] A. Jossen, V. Spath, H. Doring, J. Garche, J. Power Sources 84 (1999) 283–286.
[23] B. Ahmed, K.M.S. Nacer, N. Aziz, Energy Procedia 42 (2013) 377–386.
[24] N. Boizot, E. Busvelle, J.P. Gauthier, Automatica 46 (2010) 1483–1488.
[25] F. Xu, Y.Y. Wang, X.L. Luo, Chin. J. Chem. Eng. 21 (2013) 1038–1047.
[26] A. Johansson, A. Medvedev, Automatica 39 (2003) 909–918.